

# Double Negative Metamaterial Based on Moebius Strip

Vadym Slyusar<sup>1</sup> , Ihor Sliusar<sup>2</sup> , Sergey Sheleg<sup>3</sup> 

<sup>1</sup>Central Research Institute of Armaments and Military Equipment of Armed Forces of Ukraine, Kyiv, Ukraine, [swadim@ukr.net](mailto:swadim@ukr.net)

<sup>2</sup>Department of Information Systems and Technologies Poltava State Agrarian Academy, Poltava, Ukraine, [islyusar2007@ukr.net](mailto:islyusar2007@ukr.net)

<sup>3</sup>ENIT, Inc., Scottsdale, AZ, U.S.A., [ssheleg@yahoo.com](mailto:ssheleg@yahoo.com)

**Abstract**— The article proposes a new type of metamaterial cells (metacells) based on double Moebius strip. In this research, several design options have been considered which applied the variation of the metamaterial cells design and parameters. For their analysis, the Numerical modeling methods in Ansys EM Suite program were used due to the complexity of describing the interaction of metamaterial cells of non-Euclidean geometry with radio waves. Evaluation and comparison of proposed metacells have been held based on the following characteristics: the electric permittivity and the magnetic permeability as a function of frequency. Results of the researches have demonstrated the possibility of realization of double negative metamaterial (DNG) mode in the metamaterial cells based on the double Moebius strip. The strip width, its thickness, the interstrip gap, as well as the radius of the cylinder within which the metamaterial cell may be enabled, were used as mechanical parameters of the metacells. It is essential that 10-fold and more increase of the dimensions of metamaterial cell would be required for the obtainment of the same possibilities based on the classical split ring resonator (SRR). What concerns the entire scope of the potential ring options from among the considered ones, the ring with the internal area in the form of the Star of David provides the widest transmission band in the low frequency DNG mode. The corresponding area extends up to the transition frequency of 720 MHz. Moreover, the singular ring displays the invariance of the space orientation towards the presence of the DNG mode in low frequency region, when being used as the basis for the metacell.

**Index Terms**— double Moebius strip, metamaterial, double negative metamaterial (DNG), SRR, amplitude-frequency response, voltage standing wave ratio, VSWR.

## I. INTRODUCTION

As known, the metamaterials are the artificial composites, which characteristics exceed the limitations of the homogeneous materials and manifest the features not attributable to the material of the natural origin [1]-[3]. Such artificially structured materials are conventionally designed by means of creation of the drawing or the specific positioning of one or several materials for the widening of the range of electromagnetic properties of the microwave devices.

The resonator with the split ring (SRR) or square frame resonator [1]-[4] is used in one of the widely known metamaterials as an elementary cell. This type of the resonator enables the formation of

so called double negative metamaterial [2], [3] however, the elementary SRR resonator of relatively big dimension is needed for the obtainment of the similar effect within the low range of frequencies.

It is known, that the Moebius strip can be used as an alternative option of the design of the elementary cell. The ideas of the application of Moebius strip as the basis for the elementary cell of metamaterial have been expressed by some authors [5]-[10]. The double strip Moebius ring used as the condenser in the invention [11] is the example of the practical realization of Moebius strip design. Nevertheless, the design described in work [7] does not allow its effective application as the elementary cell of the metamaterial.

From the technical point of view, the authors of publications [5]-[10] in which the metamaterial had been proposed, consisting of the set of the elementary cells, each of which had the resonator in a form of a Moebius strip; had most closely approached the point of creation of the metamaterial based on the Moebius strip. However, not any specific constructive solutions with regard to the way of practical realization of such environment without the replacement of the basic Moebius strip by its equivalents are present in the description of the metamaterial based on Moebius strip [5]-[10].

In this regard, the purpose of the article is the closing of this gap via the review of potential designs of the metamaterial cells based on double Moebius strip.

Let's take the cell design of double negative metamaterial (DNG) proposed by the authors in patent [12] as a reference point for the further research. We will suppose that double Moebius strip is made of the conductive material. It can be metal or conductive plastic, or dielectric material coated with the conducting layer. The balance of the width, thickness of the strip as well as the distance between strips during the research process will be adjusted for the required frequency responses and aligned for the purpose of providing the needed symmetry to the ring form. The space between two strips forming the Moebius ring can be completely or partially filled with the dielectric material. In the simplest case, the air will be used as such dielectric material.

As long as both continuous and split Moebius rings can be applied in this context, we shall consistently analyze the characteristics of corresponding options of the metamaterials cells in order to compare them with one another.

## II. THE CELL OF METAMATERIAL BASED ON CONTINUOUS MOEBIUS STRIP

For the investigation of the electromagnetic properties of the considered types of metamaterial cells we shall apply models created by means of electromagnetic simulator Ansoft Electromagnetic Suite [13], [14]. According to the investigation method described in [15], [16], we shall immerse a double strip Moebius ring into the air box which also designates the borders of the metacell, and we shall use the wave port as the port for the launching of the electromagnetic waves. At that, for the purpose of the analysis of the properties of the metamaterial cells, we shall draw the diagrams of the dependence of the electric permittivity  $\epsilon$  and the magnetic permeability  $\mu$  on the frequency. In order to calculate them we will use the macros integrated into Ansoft Electromagnetic Suite, which in itself, executes

the calculations in accordance with the so-called TR method in compliance with the expressions [17]:

$$\varepsilon = \frac{n}{z}, \quad \mu = nz, \quad (1)$$

$$n = \frac{1}{kd} \arccos \left[ \frac{1}{2S_{21}} (1 - S_{11}^2 + S_{21}^2) \right], \quad (2)$$

$$z = \sqrt{\frac{(1 + S_{11})^2 - S_{21}^2}{(1 - S_{11})^2 - S_{21}^2}}, \quad (3)$$

where  $n$  – the refraction index,  $z$  – the wave impedance,  $S_{xy}$  – S-parameters of a diffusion matrix [17],  $k$  is the wave vector in free space,  $d$  – the thickness of the substrate.

As an example, the design of horizontally located continuous Moebius ring with the correlation of the strip width to the interstrip gap as 3:1 is represented in Fig. 1. The diagrams of its electric permittivity and the magnetic permeability are represented in Fig. 2, where the frequency dependence for  $\varepsilon$  is marked with the blue color, and the one for  $\mu$  is marked with the red color.

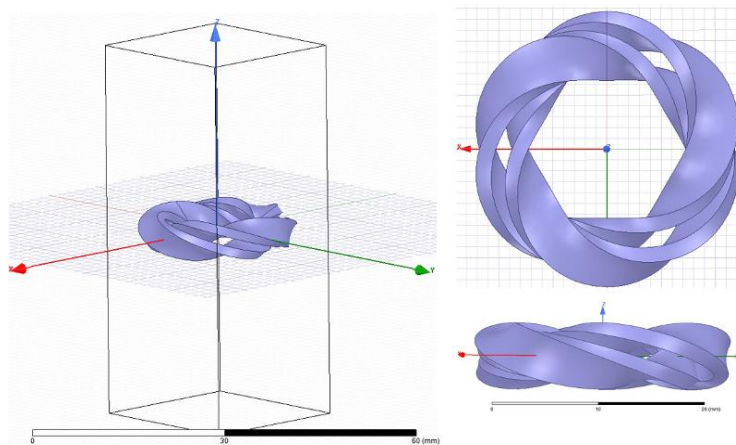


Fig. 1. The horizontally located continuous Moebius ring.

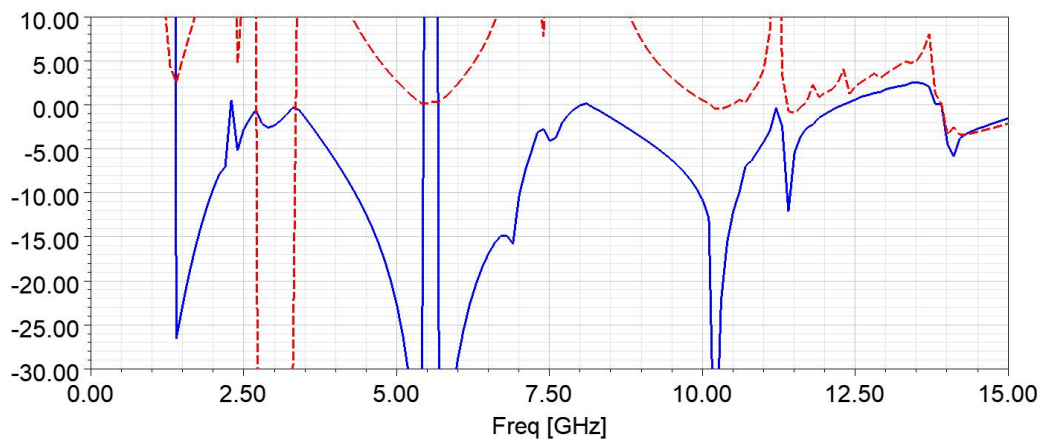


Fig. 2. The diagrams of the real components of the relative dielectric and magnetic conductivities of the cell in Fig. 1, solid -  $\text{Re}(\varepsilon)$ ; dash -  $\text{Re}(\mu)$ .

As can be seen, the cell of this design is predominantly performing in a role of  $\mu$ -negative metamaterial, but there are some DNG areas within the ranges of 3 GHz, 10 – 10.5 GHz, 11 GHz. Both electric permittivity and magnetic permeability are simultaneously negative within these areas. In this case, the application of the refraction index diagram will not enable the detection of the areas, where only the magnetic permeability is negative. That's why it is not represented herein.

In order to have the possibility to compare different options of the metacells design it is convenient (following [15], [18]-[20]) to use the concept of the relative band of DNG, which is defined by the following expression:

$$\delta F = \frac{2|f_1 - f_2|}{f_1 + f_2}, \quad (4)$$

where  $f_1$  and  $f_2$  – the border values of the frequency interval within which the metacell displays DNG properties, which means that the condition  $\{\text{Re}(\epsilon_r) < 0 \text{ and } \text{Re}(\mu) < 0\}$  is met, with  $\Delta f = f_2 - f_1$ .

The alternative vertical option of the positioning of the continuous Moebius ring in the cell, within which the wave influences its end face, is represented in Fig. 3. The corresponding frequency dependencies of real components of the electric permittivity and the magnetic permeability of the cell are represented in Fig. 4. They are remarkably similar to the diagrams of the horizontal ring, but possess the shifted frequency ranges.  $\mu$ -negative properties of the cell still prevail, but there are some DNG areas – in the regions of 4 GHz, 7.6 – 7.8 GHz; 9.3 – 10 GHz, as well as in the regions of 9.4 – 11.2 GHz, 12.4 – 13 GHz, 17.4 GHz (Fig. 4).

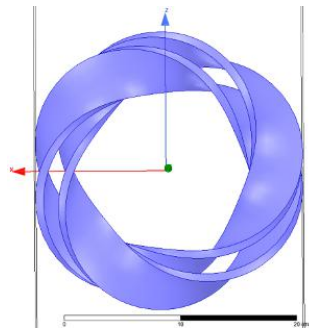


Fig. 3. The vertically positioned ring.

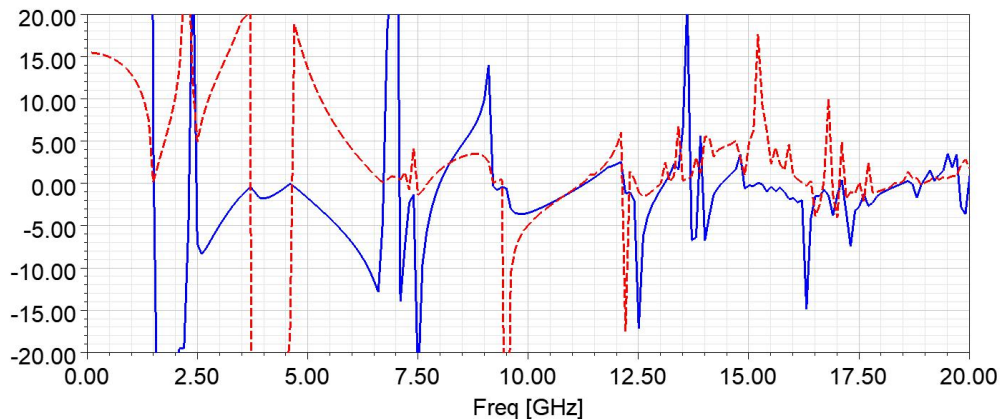


Fig. 4. The diagrams of the real components of the electric permittivity and the magnetic permeability of the cell in Fig. 3 within the frequency range up to 20 GHz, solid -  $\text{Re}(\epsilon)$ ; dash -  $\text{Re}(\mu)$ .

It should be noted for reference, that the classic option of metamaterial cell of compatible size based on the square frames [15] (Fig. 5) possesses the lower frequency band with prominent DNG properties mostly within the range of 3.3 – 4.2 GHz (Fig. 6).

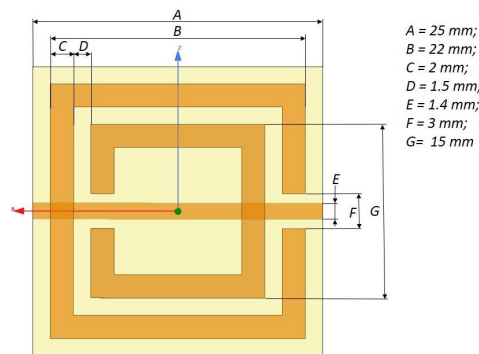


Fig. 5. The classic option of the metamaterial cell of compatible size based on the split square frames SRR [15].

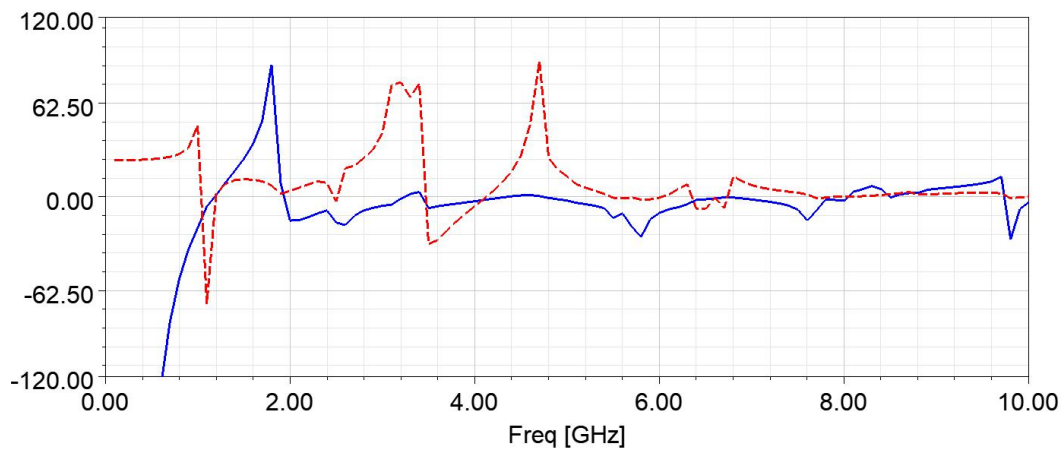


Fig. 6. The frequency band with prominent DNG properties within the range of 3.3 – 4.2 GHz of the classic cell in Fig. 5, solid -  $\text{Re}(\epsilon)$ ; dash -  $\text{Re}(\mu)$ .

The further researches of the possibilities of the cell design with the continuous Moebius strip have been aimed to the study of the influence of the particular ring parameters. One of the tested design options, which has allowed the obtainment of DNG zones within the range of 2.1 – 2.9 GHz as well as within the region of 6 GHz (Fig. 8) is represented in Fig. 7. In this case, the correlation of the strip width and interstrip gap has amounted 3:1.

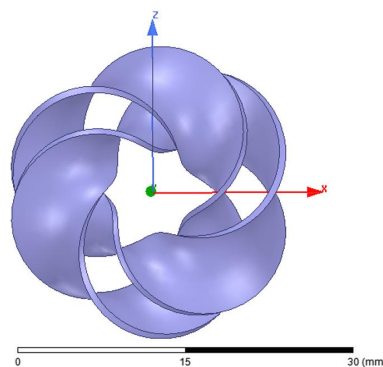


Fig. 7. The cell option with the correlation of the strip width and the interstrip gap.

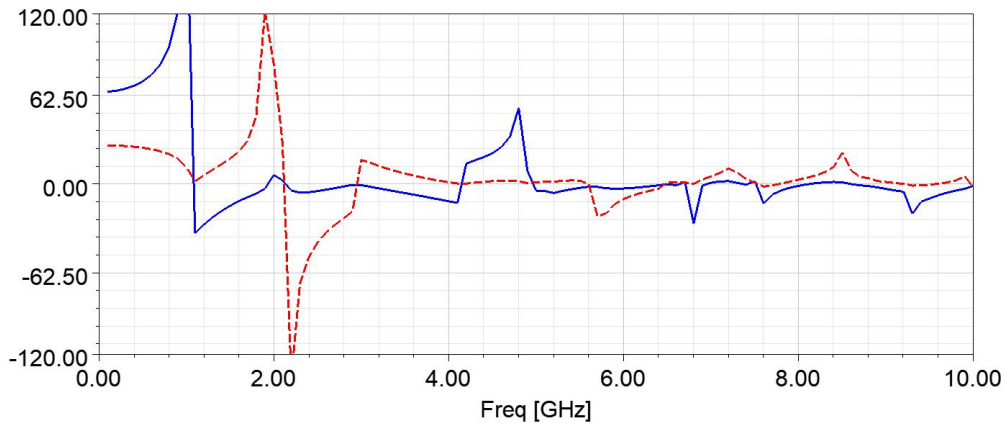


Fig. 8. The characteristics of cell in Fig. 7, solid -  $\text{Re}(\epsilon)$ ; dash -  $\text{Re}(\mu)$ .

The option with the application of the ring with the increased interstrip gap, represented in Fig. 9, has appeared to be less effective with regard to the presence of the low frequency DNG areas. Based on Fig. 10, the DNG areas appear within frequency ranges from 3.6 to 4.6 GHz, 7.6 – 8 GHz and approximately from 9 to 10 GHz. Along with it, similar to Fig. 7 and Fig. 8, only  $\epsilon$  has the negative values within the interval from 1.4 to 2.2 GHz. The present result enables the application of metamaterial with the indicated cell based on double Moebius strip for the creation of electromagnetic screens in this very area of the frequency range, where the electric permittivity is negative.

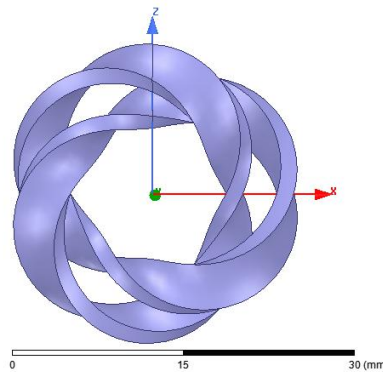


Fig. 9. The option of the ring with large interstrip gap.

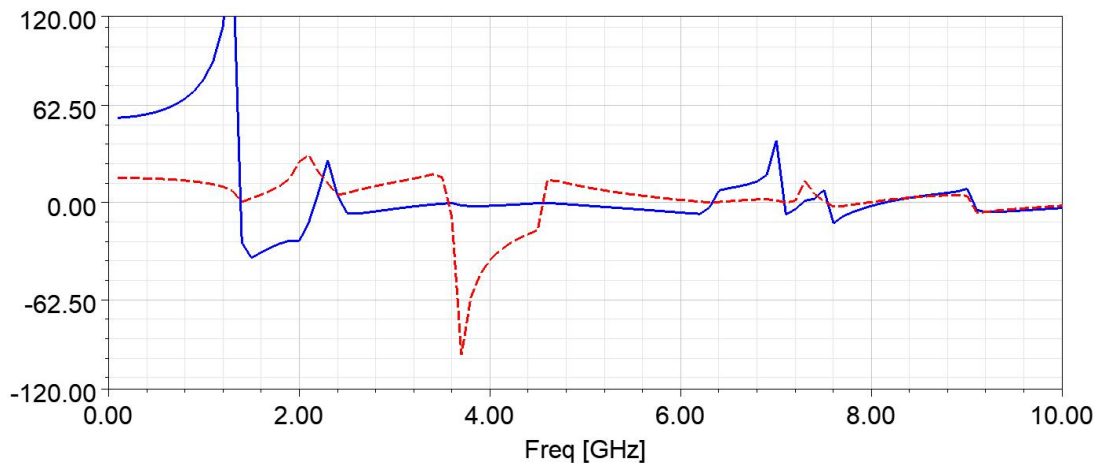


Fig. 10. The properties of the cell in Fig. 9, solid -  $\text{Re}(\epsilon)$ ; dash -  $\text{Re}(\mu)$ .

In general, it is worth noticing that the continuous Moebius ring enables the obtainment of various properties of metamaterial depending on working frequency. At that, however, the presence of DNG properties at the frequencies below 1 GHz was not fixed. The design of the cells applying the split Moebius rings, which will be revealed in the next section of the article, has appeared more effective with this regard.

### III. THE METAMATERIAL CELL BASED ON THE SPLIT MOEBIUS RING

The feature of the metamaterial cells with the split ring, distinguishing them from the options reviewed above, is the presence of the transverse strip cutout along its entire width (Fig. 11). At that, the choice of the disposition, as well as the width of the transverse cutout in the strip, as it was expected similar to [16], significantly influences the frequency range, within which the effect of the negative refraction index (DNG) takes place.

As the results of the electrodynamic modeling have displayed, the split option of Moebius ring (Fig. 11) with the outer diameter of 25.4 mm (1 inch) functions within low frequencies from 0.02 GHz to 0.54 GHz like DNG material, when the electromagnetic plane wave impacts its end face (Fig. 12). The electric permittivity and the magnetic permeability possess the negative values within this frequency domain and the value  $\delta F=1.857$ .

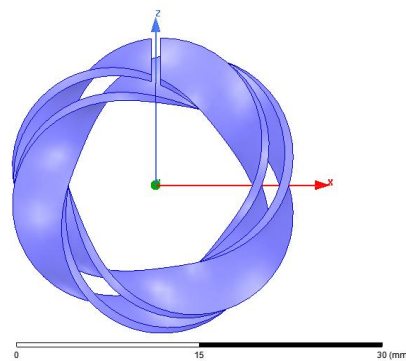


Fig. 11. The cell design with the vertical split Moebius ring.

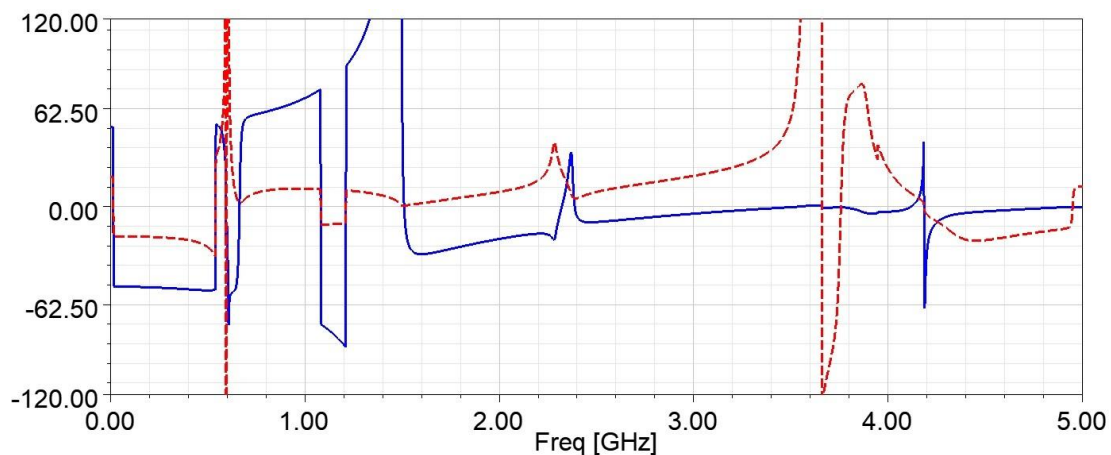


Fig. 12. The first low frequency DNG area of the cell in Fig. 11, the frequency step set to 2 MHz, solid -  $\text{Re}(\epsilon)$ ; dash -  $\text{Re}(\mu)$ .

During the rotation of the ring with the cutout directed downwards in such a way that the wave impacts the plane surface, parallel to the ring, flatwise (Fig. 13) DNG effect shifts to the frequency range of 450 – 750 MHz (Fig. 14). Moreover, DNG zone is detected within the region of 5.3 – 5.6 GHz as well, while the stable mode of ENG is possible within wide frequency range from 4.2 to 9.6 GHz.

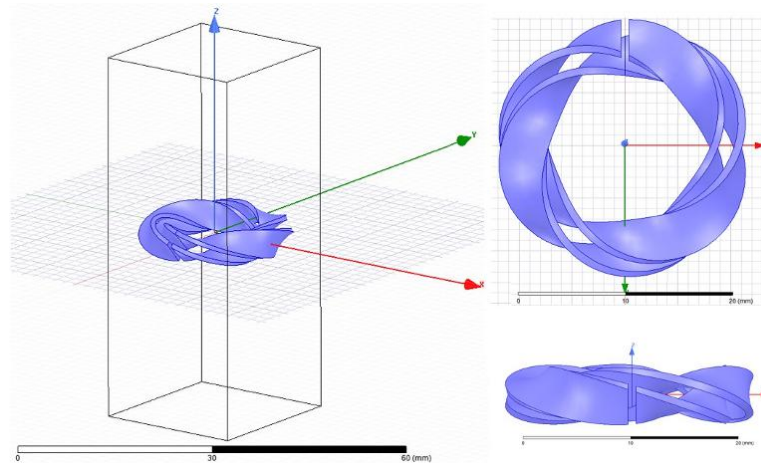


Fig. 13. The cell in a form of the horizontally positioned ring with the cutout directed downwards.

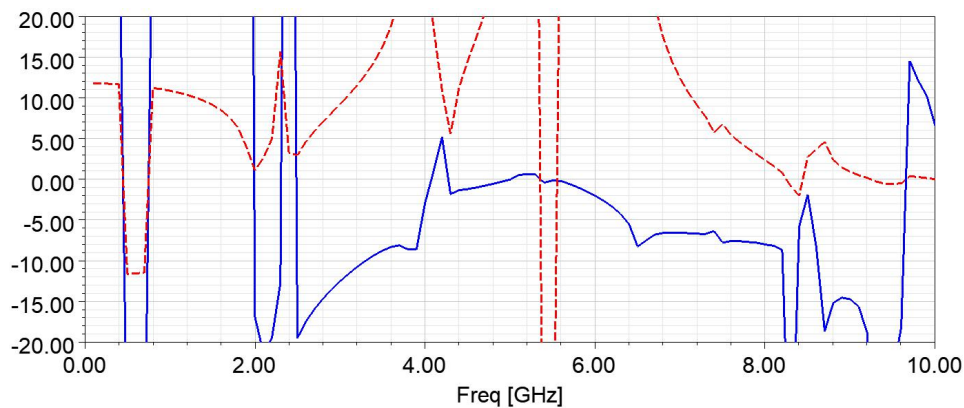


Fig. 14. Characteristics of the cell in Fig. 13, the frequency step set to 100 MHz, solid -  $\text{Re}(\epsilon)$ ; dash -  $\text{Re}(\mu)$ .

It is essential that in case of classical SRR (Fig. 5) the dimensions of SRR should be increased 10-fold (which is unacceptable) for the purpose of shift of the region with the prominent DNG properties to the frequency range similar to the specified bottom working range of the split Moebius strip.

The reviewed horizontally positioned split ring can be rotated with the cutout directed upwards (Fig. 15). The value  $\epsilon$  stays negative in this option within the region of 2 GHz (Fig. 16), as well as in the previous case (Fig. 14), on the other hand,  $\mu$  reverses sign from positive to negative within this region. It allows the obtainment of the DNG zone within specified range, as well as confirms the hypothesis that the direction of strip rotation (leftward instead of rightward in this case) impacts the sign of  $\mu$ . Thus, the working frequency range depends not only on the positioning of the cutout of Moebius strip, but also on the direction of rotation of double strip within the ring.

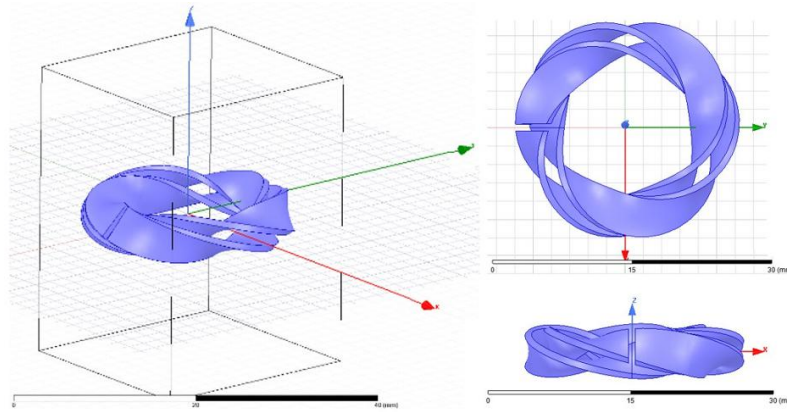


Fig. 15. The horizontally positioned split ring with the cutout directed upwards.

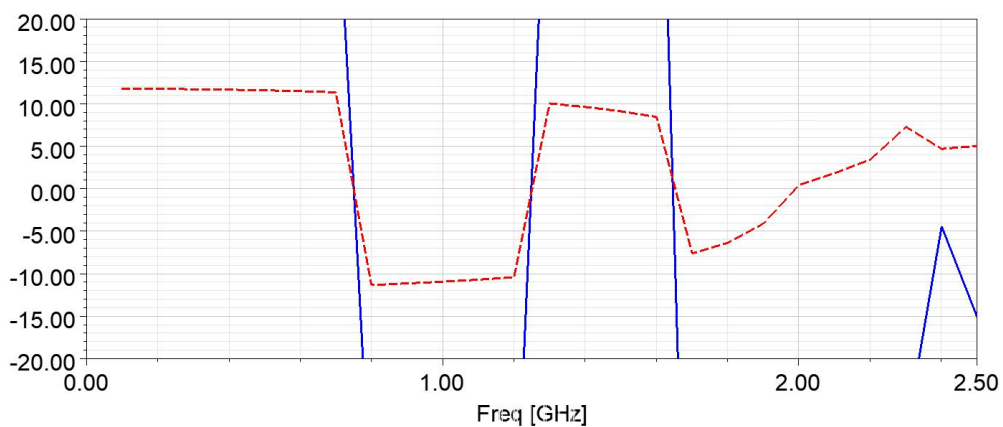


Fig. 16. DNG mode approximately from 750 to 1250 MHz and from 1.64 to 2 GHz, solid -  $\text{Re}(\epsilon)$ ; dash -  $\text{Re}(\mu)$ .

The frequency dependencies of the metamaterial properties will be somewhat different from the represented ones in case of application of the fixing elements for the fixation of Moebius strip in the cell, for example, similar to patent [12] (Fig. 17). Though DNG mode will be preserved in the area of 1.19 – 1.9 GHz (approximately 700 MHz) even in this case (Fig. 18).

For the verification of the detected regularities, the further researches have been performed with regard to the modified options of Moebius rings design. For example, for the vertical ring represented in Fig. 19, with the cutout width equal to the strip thickness, the conditions of the existence of DNG band are met within the frequency range up to 220 MHz (Fig. 20).

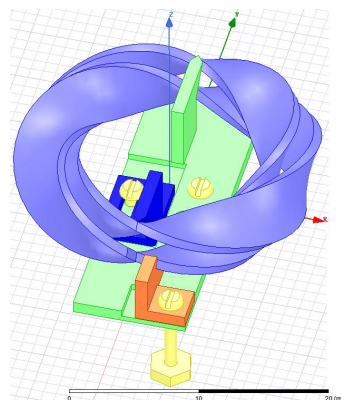


Fig. 17. The ring with the cutout in the socket with the copper contact [12].

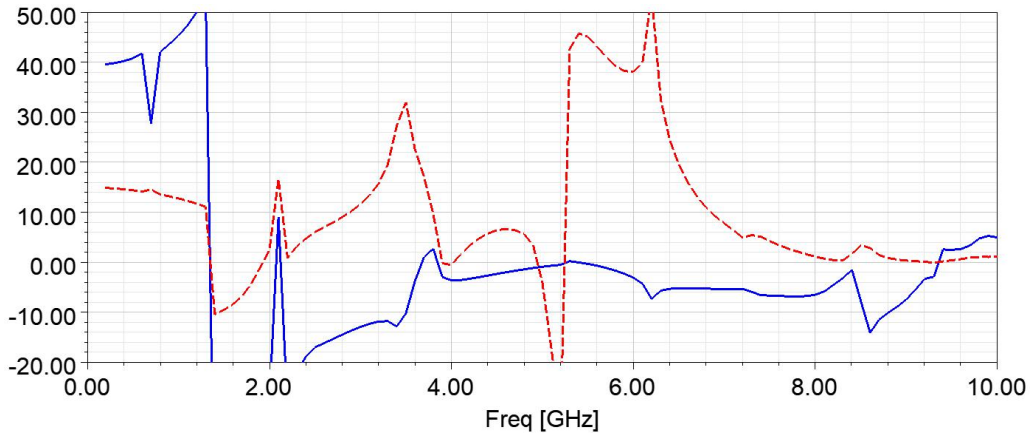


Fig. 18. The frequency properties of the cell with Moebius ring in Fig. 17, solid -  $\text{Re}(\epsilon)$ ; dash -  $\text{Re}(\mu)$ .

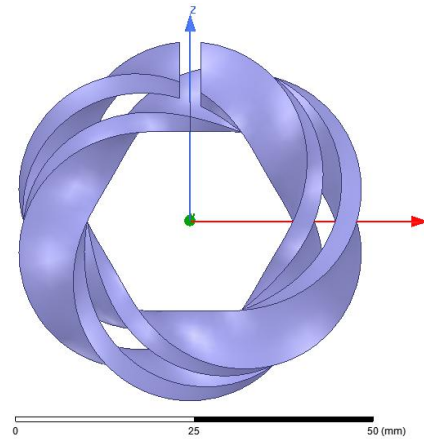


Fig. 19. Moebius ring with the pentagonal internal area.

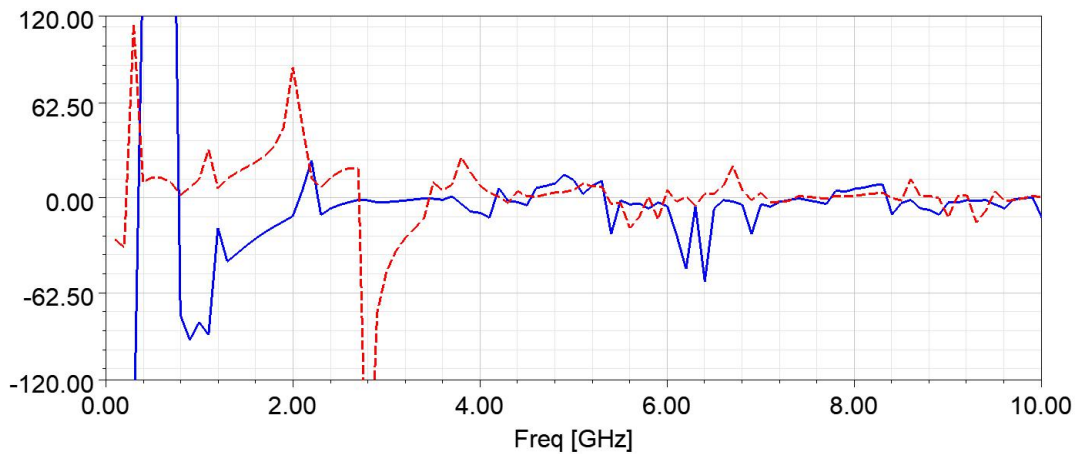


Fig. 20. DNG band up to 220 MHz, peculiar for the ring in Fig. 19, solid -  $\text{Re}(\epsilon)$ ; dash -  $\text{Re}(\mu)$ .

As it was expected, the transfer to the horizontally positioned option of the ring in Fig. 19 shifts the low frequency DNG zone to the range from 250 to 350 MHz. Electromagnetic characteristics corresponding to this design of the metamaterial cell (Fig. 21) are represented in Fig. 22.

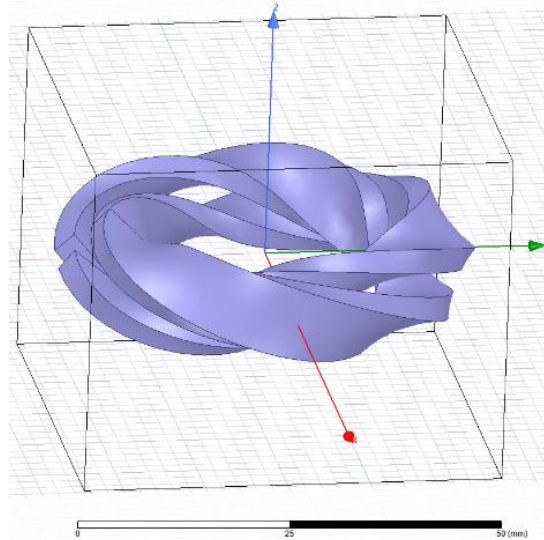


Fig. 21. The horizontal option of the ring positioning in Fig. 19.

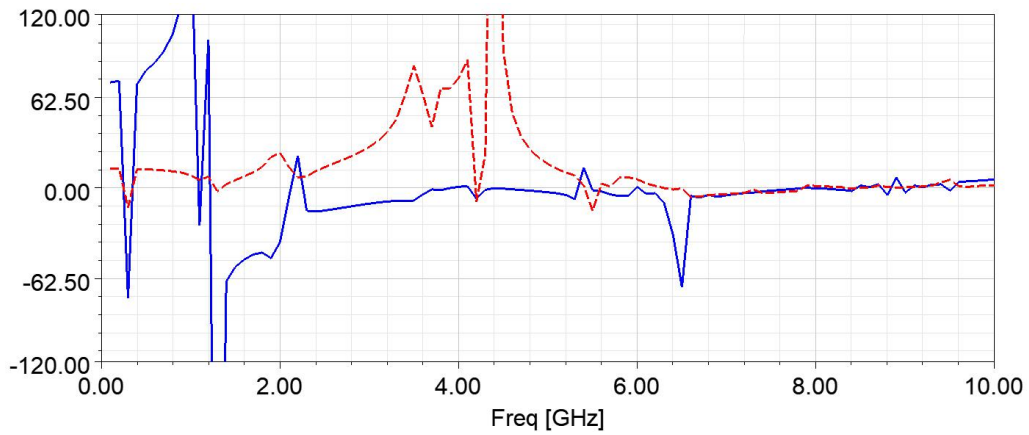


Fig. 22. The frequency properties of the cell in Fig. 21, solid -  $\text{Re}(\epsilon)$ ; dash -  $\text{Re}(\mu)$ .

The cell with the vertical ring having the internal area in a form of the Star of David (Fig. 23) displays much better frequency properties. Based on Fig. 24, DNG band exists within the frequency ranges up to 620 MHz and from 3.8 to 4.6 GHz.

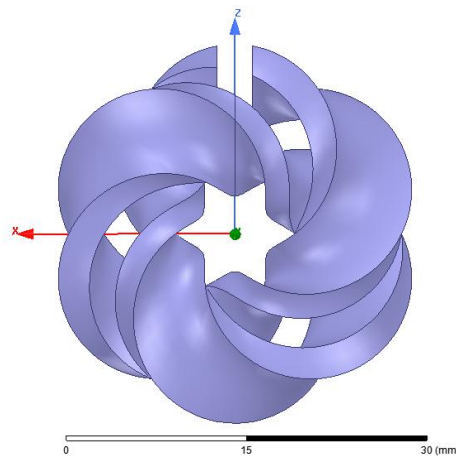


Fig. 23. The ring with the internal area in a form of the Star of David.

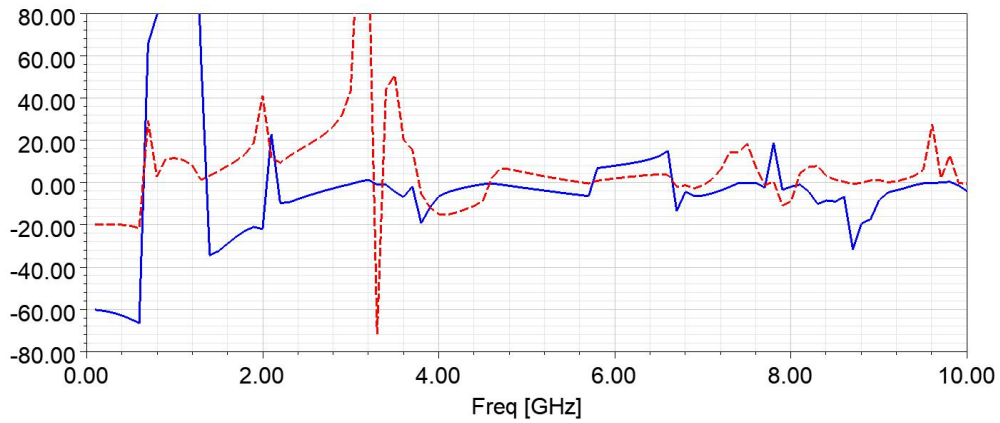


Fig. 24. The characteristics of the ring in Fig. 23, solid -  $\text{Re}(\epsilon)$ ; dash -  $\text{Re}(\mu)$ .

During the horizontal placement of this ring in the cell (Fig. 25) the low frequency DNG band shifts to the region of 500 – 600 MHz. One more DNG band is registered within the area from 550 to 750 MHz (200 MHz) and the DNG interval (640 MHz), the most extended one in terms of frequency, is located within the range of 6.56 – 7.5 GHz (Fig. 26).

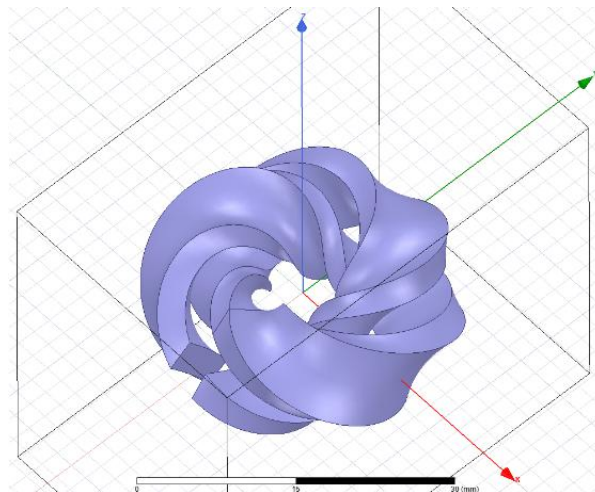


Fig. 25. The horizontally positioned ring in Fig. 23.

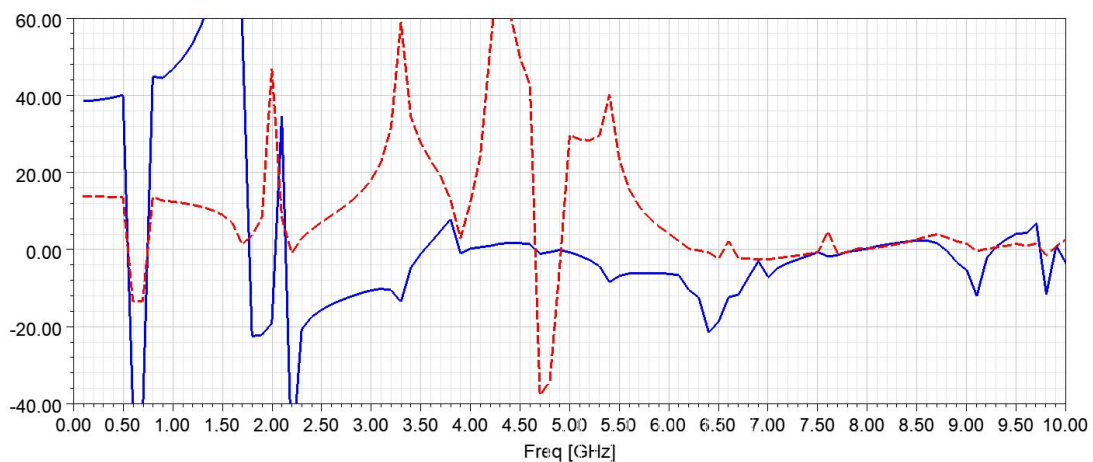


Fig. 26. The frequency properties of the cell with the ring in Fig. 25, solid -  $\text{Re}(\epsilon)$ ; dash -  $\text{Re}(\mu)$ .

Given that all reviewed design options of the metamaterial cells suggested only two variants of the orientation of Moebius ring: vertical or horizontal – it was interesting to consider the intermediate case, when the ring represented in Fig. 23 and Fig. 25 was inclined at a specific angle to the vertical plane. Particularly, let's consider the situation with the inclination of this ring at an angle of 45 degrees (Fig. 27). It turned out that such design enabled the significant extension of the low frequency DNG area in comparison with Fig. 11 and Fig. 23, shifting its cut-off frequency to the level of 720 MHz, as well as obtainment of rather wide DNG interval (900 MHz) within the range from 3.85 to 4.75 GHz (Fig. 28).

Unfortunately, the article size does not allow reviewing the manifestation of this phenomenon in the other ring options described above. Along with it, it is worth noticing that this manifestation is peculiar to them as well. This property enables the extension of the permissible angle sector within which the functioning of the metamaterial cell in DNG mode is preserved. Moreover, the requirements to the accuracy of the installation of the ring in a cell are eased.

As a confirmation of the specified regularity, we will finalize the description of the obtained results with the review of properties of the metacell based on so called singular Moebius ring [16] (Fig. 29). Its peculiar feature is the maximum possible extension of strip, forming the ring, with simultaneous preservation of fixed interstrip gap, which still allows to avoid the short circuit of the side areas of the strip due to the mutual contact [16].

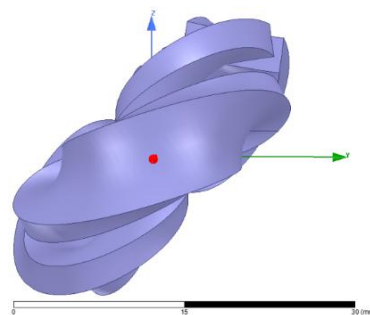


Fig. 27. Moebius ring with the inclination of 45 degrees.

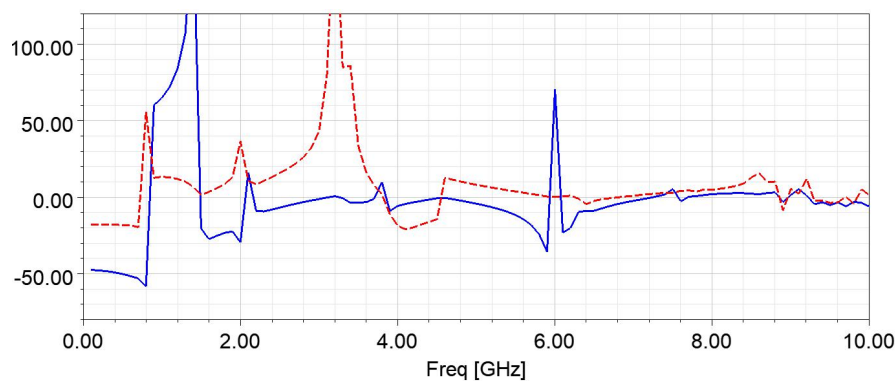


Fig. 28. The frequency dependencies of the parameters of metamaterial cell in Fig. 27 and their specific fragments with DNG areas, solid -  $\text{Re}(\epsilon)$ ; dash -  $\text{Re}(\mu)$ .

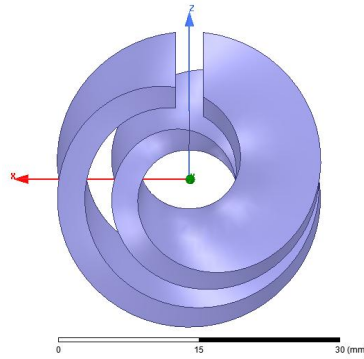


Fig. 29. The vertical singular ring with the cutout.

According to the results of modelling represented in Fig. 30, the first DNG band, which is perspective, extends up to 450 MHz (taking into account the frequency step in the simulation, equal to 100 MHz).

Unexpectedly, the best results have been provided by the horizontal ring (Fig. 31) which, unlike all previously considered options of the metacells, functions as the vertical one: DNG band is found in the bottom frequency range up to 640 MHz (Fig. 32). The second and the third DNG ranges are found from 4.01 to 4.35 GHz and from 4.45 to 5.33 GHz.

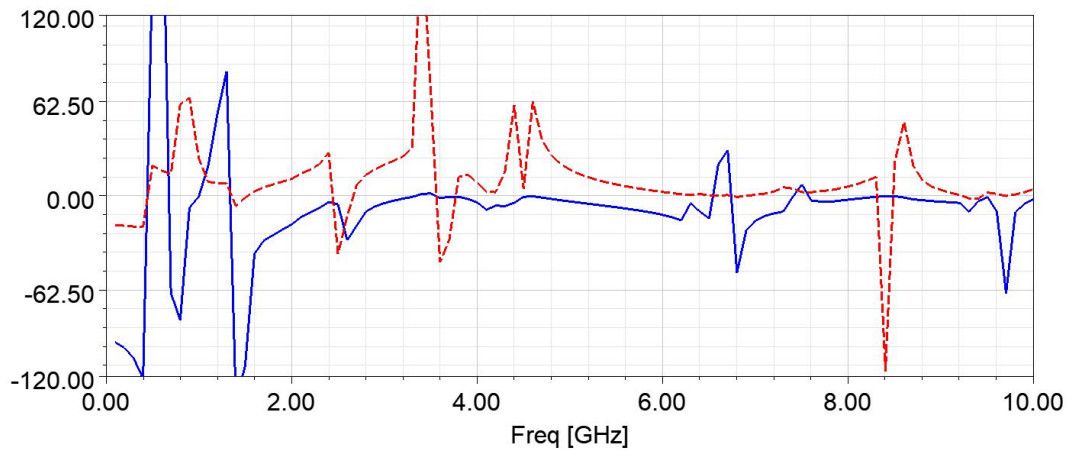


Fig. 30. The frequency properties of the vertically oriented singular ring, solid -  $\text{Re}(\epsilon)$ ; dash -  $\text{Re}(\mu)$ .

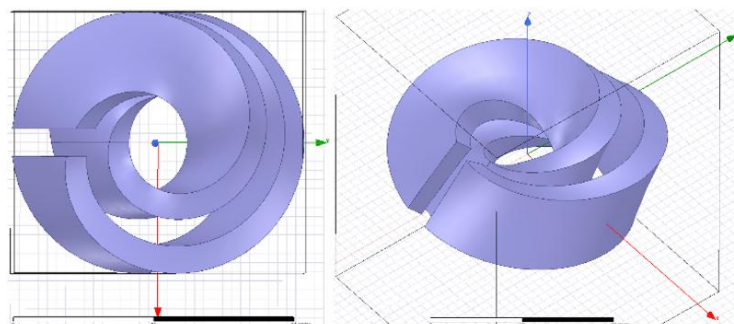


Fig. 31. The horizontally positioned singular ring.

The above defined phenomenon of the inclined ring arises in this case as well. The exterior of the corresponding metacell with the split singular ring, inclined at an angle of 45 degrees, is represented in Fig. 33. At that, the same large air box along Y axis is used, owing to which the calculation process

has slowed down significantly. The properties of the metacell with the inclined ring are represented in Fig. 34. The present ring functions similar to the vertical one – DNG band is located in the bottom frequency range up to 640 MHz. The second DNG range is within the area from 1.36 to 1.72 GHz. However, in contrast to the ring with the hole in a form of the Star of David, the increase of DNG band does not take place in this case in comparison with the vertical ring. Therefore, the invariance of the presence of low frequency DNG mode in the metacell based on singular Moebius ring towards the orientation of the ring in space, should be noted, because specific DNG area exists at any orientations of the ring. As a result, the design of the metacell based on the singular ring is the preferable choice.

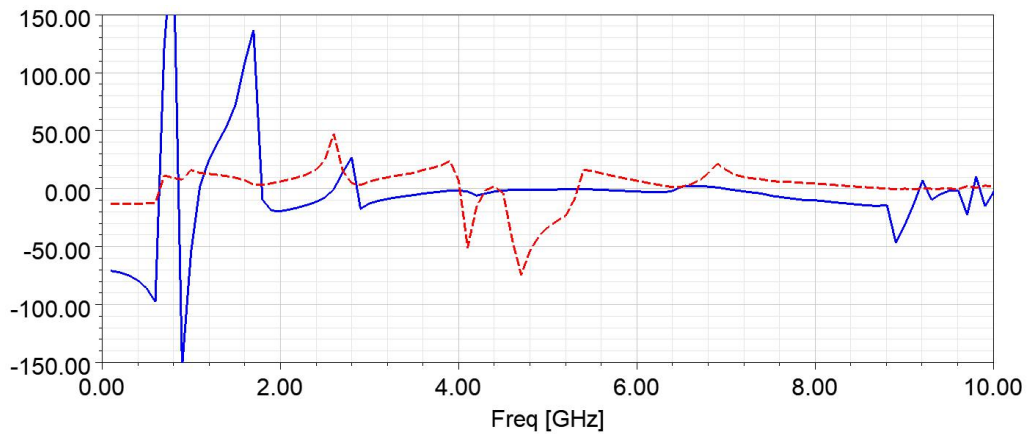


Fig. 32. The frequency properties of the horizontally positioned singular ring, solid -  $\text{Re}(\epsilon)$ ; dash -  $\text{Re}(\mu)$ .

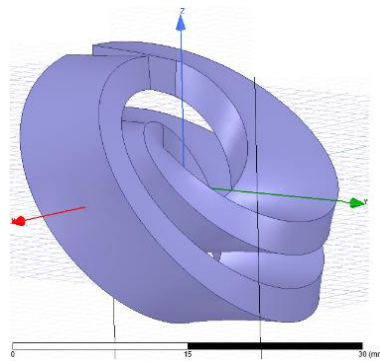


Fig. 33. Diagonally positioned singular Moebius ring.

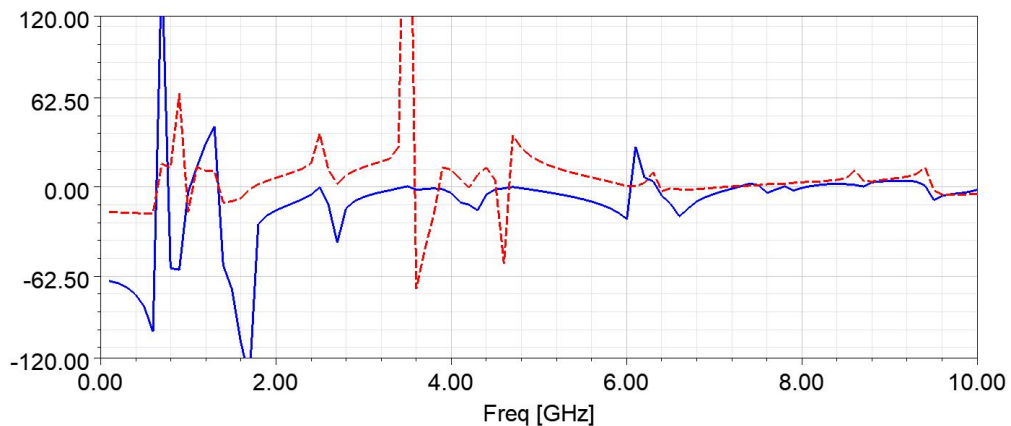


Fig. 34. The properties of the metacell with the inclined singular ring, solid -  $\text{Re}(\epsilon)$ ; dash -  $\text{Re}(\mu)$ .

What concerns the size of the air box, it can be aligned with the dimensions of the inclined ring along Y axis (Fig. 35). Such limitation of the box volume based on the ring size enables the significant acceleration of calculation process for the frequency dependences of  $\epsilon$  and  $\mu$  values, reducing it to 20 minutes within the frequency range from 0 to 10 GHz. At that, the insignificant differences in dependencies of  $\epsilon$  and  $\mu$  arise at the frequencies of up to 3 GHz (Fig. 36) in comparison with the results for the box in Fig. 33. Along with it, the differences at the higher frequency ranges are crucial. For example, at the frequency range of 8 GHz there is the surge of  $\epsilon$  value in this case, while there is none in Fig. 34.

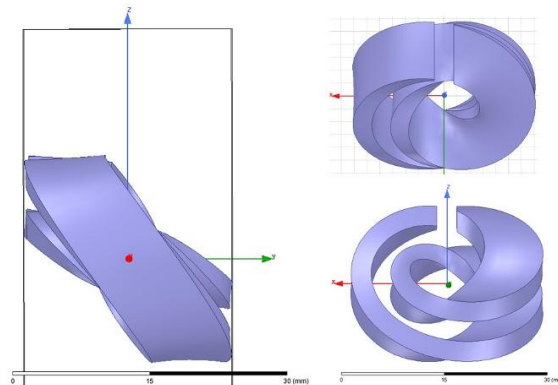


Fig. 35. The limitation of the air box volume based on the Moebius ring size.

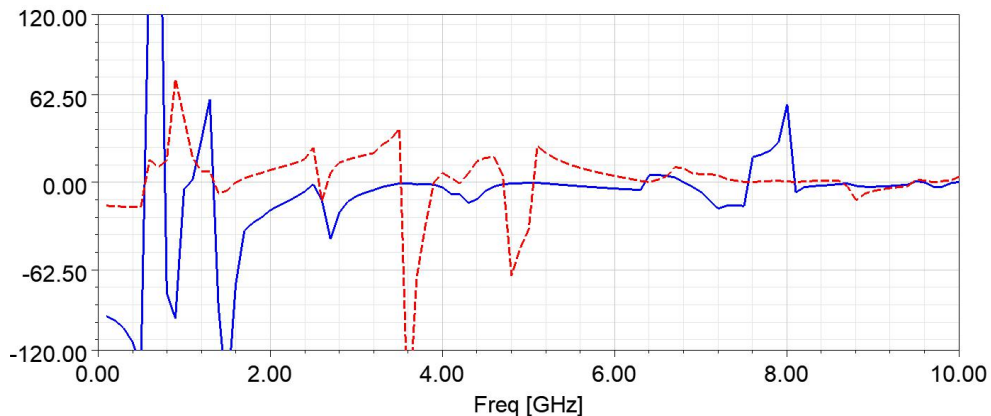


Fig. 36. The dependencies of  $\epsilon$  and  $\mu$  for the scaled down dimensions of the air box, solid -  $\text{Re}(\epsilon)$ ; dash -  $\text{Re}(\mu)$ .

The fabrication process of the proposed metacell structures can be based on additive manufacturing techniques, such as 3D printing to create physical models of antennas [16]. This may include printing metacells from various materials such as plastic, metal or ceramic with post-processing, as well as using different types of printers such as Fused Deposition Modeling (FDM) or Stereolithography (SLA). In preparing this article, several methods were tested, the results of printing the dielectric base for the subsequent galvanic coating are shown in Fig. 37 and Fig. 38. The use of non-conductive materials as the basis for a metacellular structure can have a number of advantages. One of them is that it can make the production process more economical. In addition, non-conductive materials are easier to process or shape, allowing for more precision and control in the manufacturing process. Another advantage is that dielectric materials can be lighter than conductive materials, which can be

useful in certain applications. An alternative approach is to use 3D printing to create cast molds for casting the metacell. These approaches allow for different material options, but are not covered in this work.



Fig. 36. The metacell quartet before post-processing.

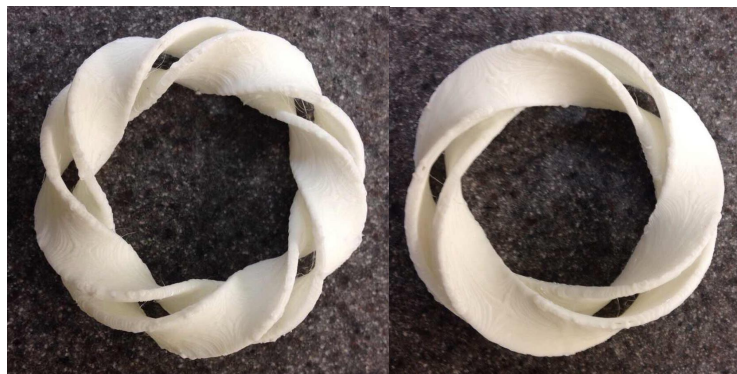


Fig. 37. The metacell variants, manufactured by means of 3D printing method after a post-processing.

#### IV. DISCUSSION

The performed researches have demonstrated the possibility of realization of DNG mode in the metamaterial cell based on the continuous Moebius ring. In conjunction with the chirality parameter, it opens up the potential for the creation of the absorbers and electromagnetic materials on their basis, absorbing and dissipating the electromagnetic waves. Along with it, the optimal effect in terms of the width of the spectral area within which the DNG properties are manifested, is demonstrated by the split Moebius rings of the reviewed topologies. For the verification of such properties in practical applications the experimental researches should be performed. At that, it makes sense to apply multi-cell modules, consisting of the several cells of the reviewed topology. The analysis of the represented frequency dependences of the electric permittivity  $\epsilon$  and the magnetic permeability  $\mu$  creates the basis for the approaching of this stage of research, enabling the selection of the best solutions for their further distribution, as well as prejudge the characteristics of the multi-cell metastructures created on

their basis. The overall properties of the metasurface will be a combination of the properties of each individual metacell. For example, if the metacells are designed to have negative values of permittivity and permeability, the metasurface will also have these properties, potentially leading to a Double Negative zone with an expanded relative frequency band. However, the specifics of how the properties of the metacells combine in the metasurface will depend on the specific design and arrangement of the metacells. On the other hand, the proposed design of metamaterial cells based on double Moebius strip can be used for the improvement of metamaterial lens [21, 22]. This approach also needs to be explored.

## V. CONCLUSION

The peculiar feature of the proposed split Moebius rings is the presence of the low frequency DNG area. It is essential that 10-fold and more increase of the dimensions of metamaterial cell would be required for the obtainment of the same possibilities based on classical SRR. The benefits of using a metacell design based on a Moebius strip include the ability to eliminate the need for a straight conductor in the metacell, making it more compact. What concerns all the potential Moebius ring options from among the considered ones, the Moebius ring with the internal area in a form of the Star of David provides the widest transmission band in the low frequency DNG mode. The corresponding area extends up to the transition frequency of 720 MHz. Moreover, the singular Moebius ring displays the invariance of the space orientation towards the presence of the DNG mode in low frequency region, when being used as the basis for the metamaterial cell. The further researches should be focused on the analysis of the maximum permissible space orientations of Moebius rings inside the cell, which will still provide the conditions for the existence of low frequency DNG area; the analysis of the efficiency of the application of several Moebius rings as the metamaterial block with various combinations of leftwards and rightwards rotations, inclination and other parameters of these rings, as well as the study of other ring designs, for example, the square topology. Moreover, the study of the influence of the cutout width in the ring, particularly, the sector form, on the electromagnetic properties of the metacell, is worth noticing.

The proposed metacells structures can be manufactured using additive manufacturing techniques, such as 3D printing. As the material for manufacturing, the authors used copper and tested various techniques, including 3D printing with post-processing and the use of conductive and dielectric materials. Alternative methods for forming metacells, such as using 3D printing to make casting molds for casting the structure, were also considered. In addition to the mentioned technological issues, options for attaching and fixing the elements of the metacells in telecommunication and radar equipment, as well as for creating arrays of metalenses were studied.

## REFERENCES

- [1] V. Veselago, "The electrodynamics of substances with simultaneously negative values of  $\epsilon$  and  $\mu$ ," *Sov. Phys. Usp.*, vol. 10, no. 4, pp. 509–514, 1968, [doi: 10.1070/PU1968v010n04ABEH003699].

- [2] V. Slyusar, "Metamaterials on antenna solutions," in *IEEE 7th Int. Conf. on Antenna Theory and Techniques (ICATT'09)*, Lviv, Ukraine, pp. 19–24, 2009.
- [3] V. Slyusar, "Metamaterials in the antenna equipment: basic principles and results," *The First Mile*, vol. 3, 4, pp. 44–60, 2010.
- [4] R. Pandeewari and S. Raghavan, "Microstrip antenna with complementary split ring resonator loaded ground plane for gain enhancement," *Microwave and Optical Technology Letters*, vol. 52, no. 2, February 2014.
- [5] A. Poddar and U. Rohde, "Metamaterial Möbius Strips (MMS): Application in Resonators for Oscillators and Synthesizers," in *2014 Proc. IEEE Int. Frequency Control Symp*, Taipei, Taiwan, May 2014, [doi:10.1109/fcs.2014.6859924].
- [6] A. Poddar, U. Rohde and T. Itoh, "Metamaterial Möbius Strips (MMS): Tunable Oscillator Circuits," in *IEEE MTT-S International Microwave Symp. (IMS 2014)*, Tampa, Florida, USA, pp. 1–4, June 2014.
- [7] U. Rohde and A. Poddar, "Möbius Strips and Metamaterial Symmetry: Theory and Applications," *Microwave Journal*, vol. 57, no. 11, pp. 76–88, November 2014.
- [8] U. Rohde and A. Poddar, "Metamaterial Möbius Strip Resonators for Tunable Oscillators," *Microwave Journal*, vol. 58, no. 1, pp. 64 – 88, January 2015.
- [9] U. Rohde and A. Poddar, "Möbius Metamaterial Inspired Next Generation Circuits and Systems," *Microwave Journal*, vol. 59, no. 5, pp. 62–90, May 2016.
- [10] U. Rohde and A. Poddar, "Möbius Metamaterial Inspired Signal Sources and Sensors," *Microwave Journal*, vol. 59, no. 6, pp. 60–94, June 2016.
- [11] T. Brown, "Möbius Capacitor," US Patent US 4599586, Dec. 8, 1982.
- [12] S. Sheleg, V. Slyusar and I. Sliusar, "Double-negative metamaterial unit cell," US Design Patent US D937777 S, Dec. 7, 2021.
- [13] S. Bankov and A. Kurushin, "Raschet antenn i SVCH struktur s pomoshchyu HFSS Ansoft [Calculation of antennas and microwave structures using HFSS Ansoft]," Moscow, Russia: ZAO NPP "Rodnik", pp. 207, 208, 2009 (In Russian).
- [14] Ansys, "3D Electromagnetic Field Simulator for RF and Wireless Design" [Online]. Available: <https://www.ansys.com/products/electronics/ansys-hfss>. [Accessed 26 May 2022].
- [15] I. Sliusar, V. Slyusar, Y. Utkin and O. Kopishynska, "Parametric synthesis of 3D structure of SRR element of the metamaterial," in *IEEE 7th Int. Sci.-Practical Conf. "Problems of Infocommunications. Science and Technology" (PICS&T'2020)*, Kharkiv, Ukraine, p. 6, October 2020, [doi:10.1109/PICST51311.2020.9468067].
- [16] V. Slyusar, I. Sliusar and S. Sheleg, "Broadband antennas based on the double Moebius strip," *Journal of Microwaves, Optoelectronics and Electromagnetic Applications*, no. 2 (21), pp. 220–241, 2022, [doi: 10.1590/2179-10742022v21i2257150].
- [17] D. Smith, D. Vier, Th. Koschny and C. Soukoulis, "Electromagnetic parameter retrieval from inhomogeneous metamaterials," *Physical Review E* 71, 036617 s2005d, pp.1–11, 2005, [doi: 10.1103/PhysRevE.71.036617].
- [18] *Assessment of Ultra-Wideband (UWB) Technology*, OSD/DARPA Ultra-Wideband Radar Review Panel, Battelle Tactical Technology Center, Contract No. DAAH01-88-C-0131, ARPA Order 6049, July 13, 1990.
- [19] I. Sliusar., V. Slyusar, S. Voloshko, A. Zinchenko and L. Degtyareva, "Synthesis of quasi-fractal ring antennas," in *IEEE 6th Int. Sci.-Practical Conf. "Problems of Infocommunications. Science and Technology" (PICS&T'2019)*, Kyiv, Ukraine, pp. 741–744, October 2019, [doi: 10.1109/PICST47496.2019.9061286].
- [20] I. Sliusar, V. Slyusar, S. Voloshko and L. Degtyareva, "Antenna synthesis based on fractal approach and DRA technologies," in *IEEE 2th Ukraine Conf. on Electrical and Computer Engineering (UKRCON-2019)*, Lviv, Ukraine, pp. 29–34, July 2019, [doi: 10.1109/UKRCON.2019.8879953].
- [21] I. V. Soares and U. C. Resende, "Radially Periodic Metasurface Lenses for Magnetic Field Collimation in Resonant Wireless Power Transfer Applications," *Journal of Microwaves, Optoelectronics and Electromagnetic Applications*, vol. 21, no. 1, pp. 48–60, March 2022, [doi: 10.1590/2179-10742022v21i1253604].
- [22] Tang, W., Chen, J. and Cui, T.J. (2021), Metamaterial Lenses and Their Applications at Microwave Frequencies. *Adv. Photonics Res.*, 2: 2100001. <https://doi.org/10.1002/adpr.202100001>.